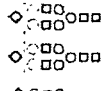
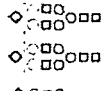
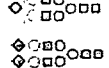
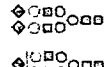
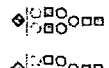
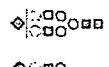
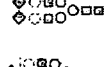
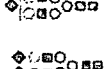

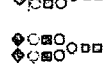
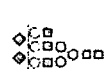
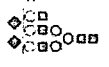


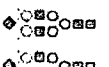
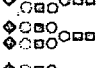
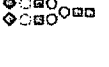
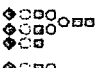
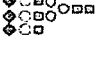
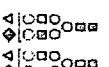
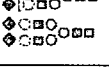

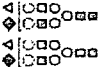
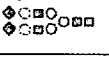



TABLE II – PUTATIVE GLYCAN STRUCTURES FROM HAPTOGLOBIN β -CHAIN, m/z VALUES, AND RELATIVE ABUNDANCE
 [COLOR TABLE CAN BE VIEWED IN THE ONLINE ISSUE, WHICH IS AVAILABLE AT WWW.INTERSCIENCE.WILEY.COM.]

Peak No	m/z	Glycan structure		Relative abundance		
				Prostate cancer	Benign prostate	Normal subject
A: NLFLNHSENATAK(203-215)¹						
1	5286.8 ± 9.0	[NeuAc1Hex2HexNAc2+Man3GlcNAc2] + [NeuAc1Hex2HexNAc2+Man3GlcNAc2]]		ND	9.6	17.8
2	5576.9 ± 15.0	[NeuAc1Hex2HexNAc2+Man3GlcNAc2] + [NeuAc2Hex2HexNAc2+Man3GlcNAc2]		10.5	22.3	31.1
3	5870.5 ± 17.0	[NeuAc2Hex2HexNAc2+Man3GlcNAc2] + [NeuAc2Hex2HexNAc2+Man3GlcNAc2]]		12.8	14.3	12.5
4	5941.7 ± 18.0	[NeuAc1Hex2HexNAc2+Man3GlcNAc2] + [NeuAc2Hex3HexNAc3+Man3GlcNAc2]		4.3	7.3	11.0
5	6235.1 ± 18.0	[NeuAc1Hex2HexNAc2+Man3GlcNAc2] + [NeuAc3Hex3HexNAc3+Man3GlcNAc2] [NeuAc2Hex2HexNAc2+Man3GlcNAc2] + [NeuAc2Hex3HexNAc3+Man3GlcNAc2]		17.0	17.0	9.2
6	6381.5 ± 18.0	[NeuAc1Hex2HexNAc2+Man3GlcNAc2] + [NeuAc3Hex3HexNAc3+Man3GlcNAc2 + Fuc]		6.7	8.2	5.8
7	6525.4 ± 18.0	[NeuAc2Hex2HexNAc2+Man3GlcNAc2] + [NeuAc3Hex3HexNAc3+Man3GlcNAc2]]		14.7	6.4	6.0
8	6597.3 ± 17.0	[NeuAc2Hex3HexNAc3+Man3GlcNAc2] + [NeuAc2Hex3HexNAc3+Man3GlcNAc2]]		4.4	3.3	6.6
9	6668.2 ± 18.0	[NeuAc2Hex3HexNAc3+Man3GlcNAc2] + [NeuAc2Hex3HexNAc3+Man3GlcNAc2 + Fuc]		7.3	4.1	ND
10	6891.6 ± 18.0	[NeuAc2Hex3HexNAc3+Man3GlcNAc2] + [NeuAc3Hex3HexNAc3+Man3GlcNAc2]]		7.3	3.4	ND
11	7034.6 ± 17.0	[NeuAc2Hex3HexNAc3+Man3GlcNAc2] + [NeuAc3Hex3HexNAc3+Man3GlcNAc2 + Fuc]		4.5	4.1	ND
12	7182.4 ± 20.0	[NeuAc3Hex3HexNAc3+Man3GlcNAc2] + [NeuAc3Hex3HexNAc3+Man3GlcNAc2]]		6.3	ND	ND
13	7328.9 ± 20.0	[NeuAc3Hex3HexNAc3+Man3GlcNAc2] + [NeuAc3Hex3HexNAc3+Man3GlcNAc2 + Fuc]		4.2	ND	ND
				100.0	100.0	100.0
B: VVLHPNYSQVDIGLIK (236-251)²						
1'	3611.7 ± 9.0	[NeuAc1Hex2HexNAc2+Man3GlcNAc2] - 98 (N-terminal Val residue?)		8.8	11.2	ND
1	3711.4 ± 9.0	[NeuAc1Hex2HexNAc2+Man3GlcNAc2]		10.6	8.0	ND
2'	3906.2 ± 9.0	[NeuAc2Hex2HexNAc2+Man3GlcNAc2] - 98 (N-terminal Val residue?)		28.4	25.9	ND
2	4004.6 ± 9.0	[NeuAc2Hex2HexNAc2+Man3GlcNAc2]		35.5	30.0	ND
2*	4132.5 ± 15.0	[NeuAc2Hex2HexNAc2+Man3GlcNAc2] + 128		4.5	11.6	ND
2**	4278.9 ± 15.0	[NeuAc2Hex2HexNAc2+Man3GlcNAc2] + 128 + 146 (Fuc?)		2.1	8.6	ND
3'	4554.8 ± 18.0	[NeuAc3Hex3HexNAc3+Man3GlcNAc2] - 102 (N-terminal Val residue?)		5.5	4.7	ND
3	4657.1 ± 18.0	[NeuAc3Hex3HexNAc3+Man3GlcNAc2]		4.6	ND	ND
				100.0	100.0	
C: MVSHHNLTTGATLINEQWLLTTAK(179-202)³						
1	4641.8 ± 9.0	[NeuAc1Hex2HexNAc2+Man3GlcNAc2]]		14.2	16.5	ND
2	4783.1 ± 15.0	[NeuAc1Hex2HexNAc2+Man3GlcNAc2 + Fuc]		21.1	27.5	ND
3	4931.9 ± 17.0	[NeuAc2Hex2HexNAc2+Man3GlcNAc2]]		64.7	56.0	ND
				100	100	

ND: not determined, due to limited sample availability.

¹N-207 & 211, MW1458.735; ²N-241, MW1795.0112; ³N-184, MW2679.3923.

ture from the respective molecular ions (m/z 1,969 and m/z 2,780 in Figs. 5a and 5b, respectively). Similar analysis of the difucosylated tri-antennary glycan at m/z 3,952 showed that this glycan predominantly carries 2 SLe^a or SLe^b antennae (Fig. 5c). No signals were observed consistent with alternative fucosylation of any

of these glycans, although we cannot rule out minor core fucosylation because there are relatively high levels of background noise in the vicinity of the m/z values corresponding to loss of the reducing end sugar (for example, m/z 2,690 and 3,501 in Figs. 5a and 5b, respectively).

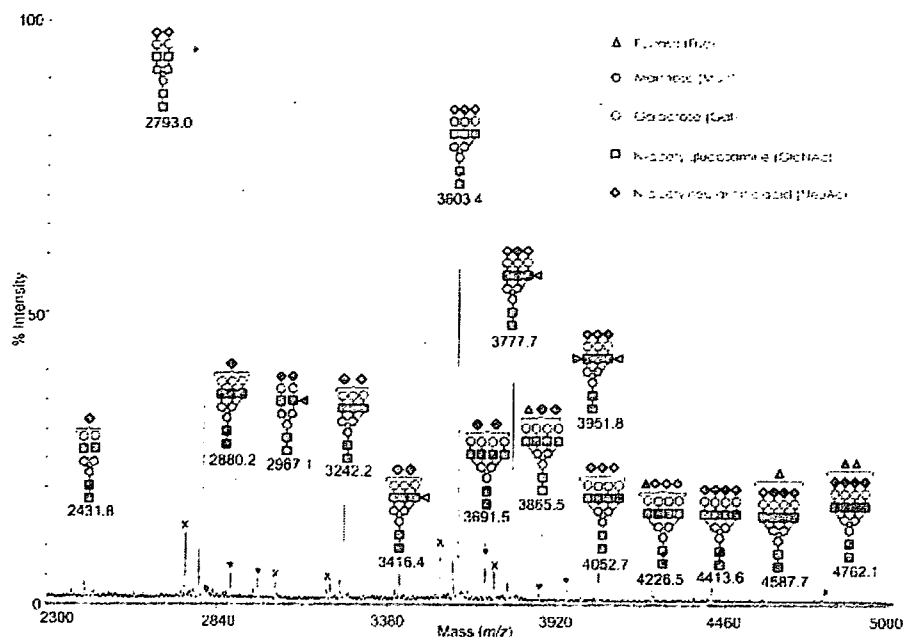


FIGURE 4 – MALDI-TOF spectra of prostate cancer haptoglobin *N*-glycans. Glycans were released by PNGase-F, permethylated, and subjected to Sep-Pak cleanup (“Material and methods”). Data from one of the fractions collected upon SepPak cleanup are shown. Cartoon assignments are based on the precise fit between composition calculations and the m/z ($z = 1$) ratio of the molecular ions detected. These cartoons represent the most likely structures taking into account the biosynthetic pathways and, when available, MALDI TOF/TOF MS/MS data. Each of the major peaks presents a minor peak distant by 14 mass units that corresponds to an under-methylated species. Ions labeled with a cross correspond to permethylation artifacts. [Color figure can be viewed in the online issue, which is available at www.interscience.wiley.com.]

To search for the possible presence of glycans containing RM2-related epitopes,¹⁶ we calculated m/z values for bi- and tri-antennary glycans carrying 1 or more RM2 sequences and/or its disialylated sub-structure (Table III). None of these m/z values was found to be more abundant than the background noise. We know from other studies in our laboratory that minor molecular ions which are hidden in the background are frequently observed in MS/MS experiments because of lower background noise. Therefore, we selected each of the calculated m/z values in Table III for MS/MS analysis, together with observed molecular ions at similar masses, which served as controls for sensitivity of detection of fragment ions. Excellent MS/MS data were obtained on all the visible molecular ions in the vicinity of the calculated m/z values, *i.e.*, from m/z 3,100 up to m/z 4,200, and these components are annotated in Figure 4. In contrast, no fragment ions consistent with sialylated glycans were obtained when any of the calculated m/z values given in Table III were selected.

Reductive elimination experiments reveal some *O*-glycosylation in prostate cancer haptoglobin

Having failed to detect the RM2 structure on the *N*-glycans of haptoglobin, we investigated the possibility that haptoglobin might be *O*-glycosylated, and that the RM2 epitope might be associated with this class of glycans. Although *O*-glycans have not previously been found in haptoglobin, NetOGlyc (<http://www.cbs.etu.dk/services/NetOGlyc/>) analysis of the haptoglobin sequence indicates that some sites in both the β - and α -chains are favorable for *O*-glycosylation. To search for putative *O*-glycans, the gel-purified β - and α 2-chains of prostate cancer haptoglobin (Fig. 1c) were subjected to reductive elimination followed by permethylation and MS analysis. Reductive elimination is known to efficiently release *O*-glycans from glycoproteins, and this treatment also partially releases *N*-glycans. Thus, the presence and the

abundance of *N*-glycans in the resulting mass spectra serve as a control for the efficiency of the reaction.

Figure 6 shows the MALDI-MS profile obtained for the purified β -chain. In the total spectrum (Fig. 6a), the 2 major *N*-glycan structures are annotated. The m/z region corresponding to molecular ions consistent with *O*-glycan structures have been magnified (Fig. 6b). Two molecular ions corresponding to sialylated core Type 1 *O*-glycans have been assigned (m/z 895 and 1,256). However, the high background in the vicinity of these 2 ions, and their low abundance, prevent their unequivocal identification. Therefore, these ions were subjected to MS/MS analysis. For both ions, characteristic fragment ions consistent with the loss of sialic acid residues (m/z 520, and m/z 881 and 472) confirmed the presence of mono- and disialylated core Type 1 *O*-glycans (Figs. 7a and 7b, respectively). Very similar results were obtained from analysis of the purified α 2-chain of prostate cancer haptoglobin (data not shown).

Having discovered that *O*-glycans are indeed present on prostate cancer haptoglobin, albeit at very low levels, we searched for RM2-related epitopes on this family of glycans. Following the same strategy as the 1 used for *N*-glycans, m/z values corresponding to predicted core Type 1 and core Type 2 *O*-glycan sequences carrying RM2 and di-sialylated epitopes were subjected to MS/MS analysis. No evidence for such structures was found using this methodology, despite excellent data being acquired for several very minor *N*-glycans of similar m/z values (data not shown).

Discussion

This study has addressed the following aspects of serum haptoglobin of patients with prostate cancer vs. benign prostate disease, and normal subjects: (i) changes of haptoglobin level; (ii) differences in *N*-glycosylation level and *N*-glycan structures; (iii) haptoglobin as a possible carrier of the RM2 epitope which was previ-

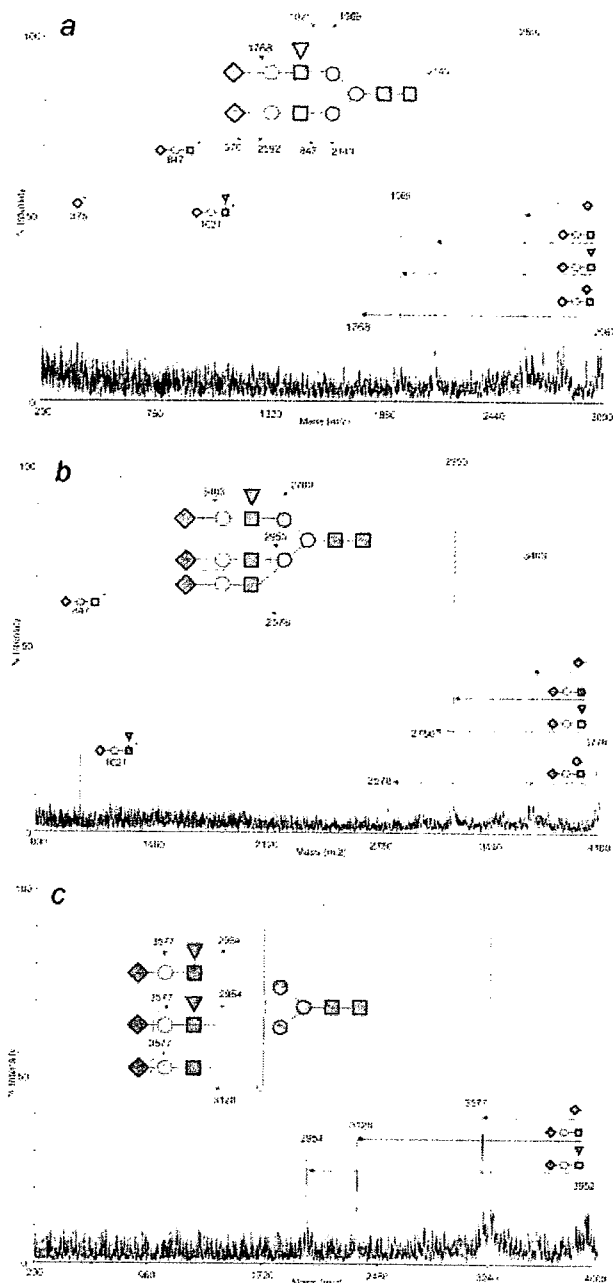


FIGURE 5 – MALDI-TOF/TOF MS/MS spectra of m/z 2,967 (a), m/z 3,778 (b) and m/z 3,952 (c) *N*-glycans from prostate cancer haptoglobin. In each of the 3 panels, the major component is shown in the schematic. Fucose residue(s) are located on the antennae as demonstrated by the presence of fragment ion at m/z 1,021 (a and b) and/or by the presence of an ion corresponding to the loss of this structure (m/z 2,954, c). For keys, see Figure 2 [Color figure can be viewed in the online issue, which is available at www.interscience.wiley.com.]

ously suggested to be enhanced specifically in prostate cancer; (iv) the possible presence of *O*-glycans.

The expression of haptoglobin was found to be significantly elevated in the sera of prostate cancer patients compared to benign prostate disease patients and normal subjects. This is consistent with many previous observations on increased levels of acute

phase proteins such as haptoglobin in the sera of patients with inflammatory diseases and cancer.^{19,30,31} This may be due to the epithelial-mesenchymal transition phenomenon. Furthermore, actively-growing tumor cells show many similar properties to inflammatory cells, particularly activated fibroblasts.^{32,33}

Based on our structural studies of haptoglobin, we conclude the following: (i) Bi-antennary mono- and disialylated glycans are common to all samples and were the major structures observed at all *N*-glycosylation sites. Significantly, tri-antennary structures together with a few tetra-antennary structures were also found, particularly at N207 and N211, and their levels were higher in prostate cancer samples than in benign prostate disease or normal samples. (ii) Fucosylated glycans were most abundant in the prostate cancer sample. (iii) The fucoses were found to be mainly on the antenna(e) rather than the cores of the *N*-glycans. This was rigorously established by MALDI-TOF-TOF MS/MS analysis of permethylated glycans. (iv) No *N*-glycans carrying the RM2 epitope or its analogue were detected, despite careful searches using highly sensitive mass spectrometric methodologies available. (v) In an attempt to explain the RM2 cross-reactivity of prostate cancer haptoglobin, we investigated the possible presence of *O*-glycans, since the Cad epitope was proposed as O-linked,³⁴ and both Cad and disialyl-Le^x (FH9) epitope⁹ have close homology with RM2. High sensitivity MS/MS analysis provided unambiguous evidence for low levels of *O*-glycosylation. This is the first observation that O-linked structures are present in haptoglobin. However, the glycans detected were mono- and disialylated core Type 1 structures, and no evidence was found for RM2 or analogous sequences such as Cad. In summary, despite extensive searches for the presence of RM2 and Cad sequences in the *N*- and *O*-glycans in haptoglobin, none was detected. Thus, the possible presence of RM2 epitopes in prostate cancer haptoglobin, as suggested through antibody staining studies (Saito et al., unpublished data), has not been confirmed by rigorous structural analysis, *i.e.*, glycosyl epitope originally assigned as GalNAc β 4-disialyl-Lc4 or its analogue is not detectable in haptoglobin. The specific structural attributes of prostate cancer haptoglobin that result in cross-reactivity with RM2 antibodies remain to be determined. It should be noted that mAbs (often IgM, less frequently IgG3) directed to disialyl glycosyl epitopes display “polyreactivity” with related or unrelated structures, surprisingly including actin, thyroglobulin, tubulin, DNA (particularly single-stranded).³⁵ mAb RM2 may react with unknown, non-carbohydrate structures associated with haptoglobin.

Over the past 20 years, many laboratories have investigated the levels and glycosylation patterns of serum haptoglobin from a range of cancers, including ovarian, breast, small cell lung, pancreatic and liver cancers, hoping to identify specific markers that might be suitable for diagnostic assays.^{30,36–40} Over-expression of haptoglobin, and changes in the level of fucose and/or sialic acid residues, are common themes emerging from all these studies, but no cancer-specific glycoform of haptoglobin has been found to date. Our studies of prostate cancer haptoglobin have opened up 2 new avenues for investigation. First, the detection of *O*-glycans in haptoglobin is potentially an important observation because *O*-glycans have been identified as the major *in vivo* ligands for selectins. Moreover, there is evidence pointing to physiological regulation of *O*-glycosylation, notably in pregnancy.⁴¹ It will be interesting, therefore, to characterize *O*-glycosylation of haptoglobin in ovarian and breast cancers. Second, our experiments have provided the first rigorous discrimination of core and antenna fucosylation in haptoglobin. Most of the previous studies employed lectins to probe changes in fucosylation, with consequent uncertainty in the precise fucosylation pattern. In those instances where more rigorous mass spectrometric methods were used, for example in the pancreatic cancer study,⁴⁰ the authors were unable to unambiguously establish the fucosylation sites in many of the glycans, particularly the multi-antennary components. Interestingly, in all previous studies where sites of fucosylation have been reported, increases in core fucosylation were observed, whereas antenna

TABLE III – POTENTIAL STRUCTURES FOR RM2 AND CAD EPTOPE
[COLOR TABLE CAN BE VIEWED IN THE ONLINE ISSUE, WHICH IS AVAILABLE AT WWW.INTERSCIENCE.WILEY.COM.]

Potential structures with RM2 epitope			Potential structures with Cad epitope		
<i>m/z</i>	Structures	Composition	<i>m/z</i>	Structures	Composition
3398		Hex ₅ HexNAC ₅ NeuAc ₃ +Na ⁺	3153		Hex ₅ HexNAC ₄ NeuAc ₃ +Na ⁺
4004		Hex ₅ HexNAC ₆ NeuAc ₄ +Na ⁺	3514		Hex ₅ HexNAC ₄ NeuAc ₄ +Na ⁺
4208		Hex ₆ HexNAC ₆ NeuAc ₄ +Na ⁺	3963		Hex ₆ HexNAC ₅ NeuAc ₄ +Na ⁺

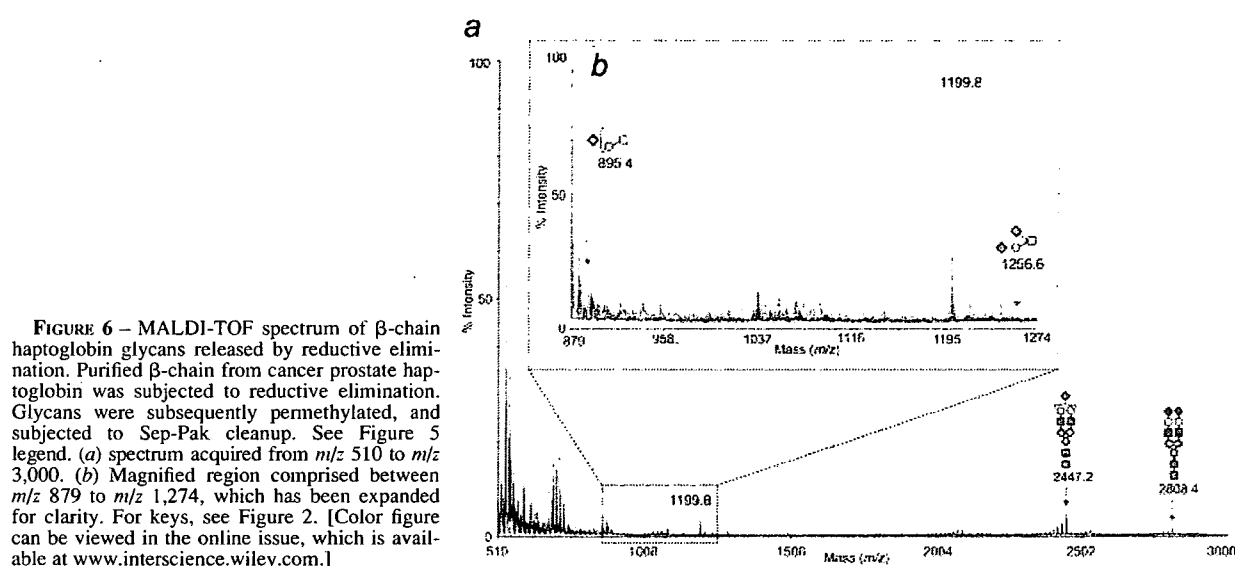


FIGURE 6 – MALDI-TOF spectrum of β -chain haptoglobin glycans released by reductive elimination. Purified β -chain from cancer prostate haptoglobin was subjected to reductive elimination. Glycans were subsequently permethylated, and subjected to Sep-Pak cleanup. See Figure 5 legend. (a) spectrum acquired from *m/z* 510 to *m/z* 3,000. (b) Magnified region comprised between *m/z* 879 to *m/z* 1,274, which has been expanded for clarity. For keys, see Figure 2. [Color figure can be viewed in the online issue, which is available at www.interscience.wiley.com.]

fucosylation was not always reported. In contrast, we observed significant levels of antenna fucosylation in prostate cancer haptoglobin, but core fucosylation was not detected. We suggest that quantitative comparisons of core versus antenna fucosylation of haptoglobin from different cancers might yield useful information for diagnostic purposes.

The presence of multi-antennary *N*-glycans (tri-antennary or more) is common not only in haptoglobin in prostate cancer (present study) and pancreas cancer,⁴⁰ but also in many other glycoproteins expressed in transformed cells. Compared to normal cells, transformed cells were found to express glycans with higher molecular mass.⁴² Moreover, multi-antennary glycans were observed to be closely associated with oncogenic transformation^{43,44} and have been suggested to be potential prognoses for cancer development and metastasis.⁴⁵

Haptoglobin *N*-glycans from prostate cancer may be qualitatively different from those of benign prostate disease or normal subjects, if expression of multi-antennary *N*-linked structures with SLe^x/SLe^a at a defined site of haptoglobin β -chain is characteristic of prostate cancer. Therefore, combinations of antibodies

directed to haptoglobin β -chain, *Phaseolus vulgaris*-L lectin (which reacts specifically with the β 1-6GlcNAc branch common to tri- or tetra-antennary but not bi-antennary structure),^{46,47} and antibodies directed to SLe^x/SLe^a, may provide diagnostic tools for prostate cancer.

Conversion of bi-antennary to multi-antennary structures, due to enhanced GlcNAc transferase-V, is generally accepted as a common phenotype, directly or indirectly controlled by oncogenes.^{48–50} Expression of multi-antennary *N*-linked structures with modified fucosylation may be a common denominator in basic cancer-associated changes in haptoglobin. Further extensive glycomic studies will help clarify the relationship between glycosylation changes and disease progression in general.

Acknowledgements

A.D. is a BBSRC Professorial Fellow. B.T. was supported by a Research Councils UK Basic Technology Grant (GR/S79268). P.-C.P. was supported by a Malaysian Perdana Scholarship and by Imperial College.

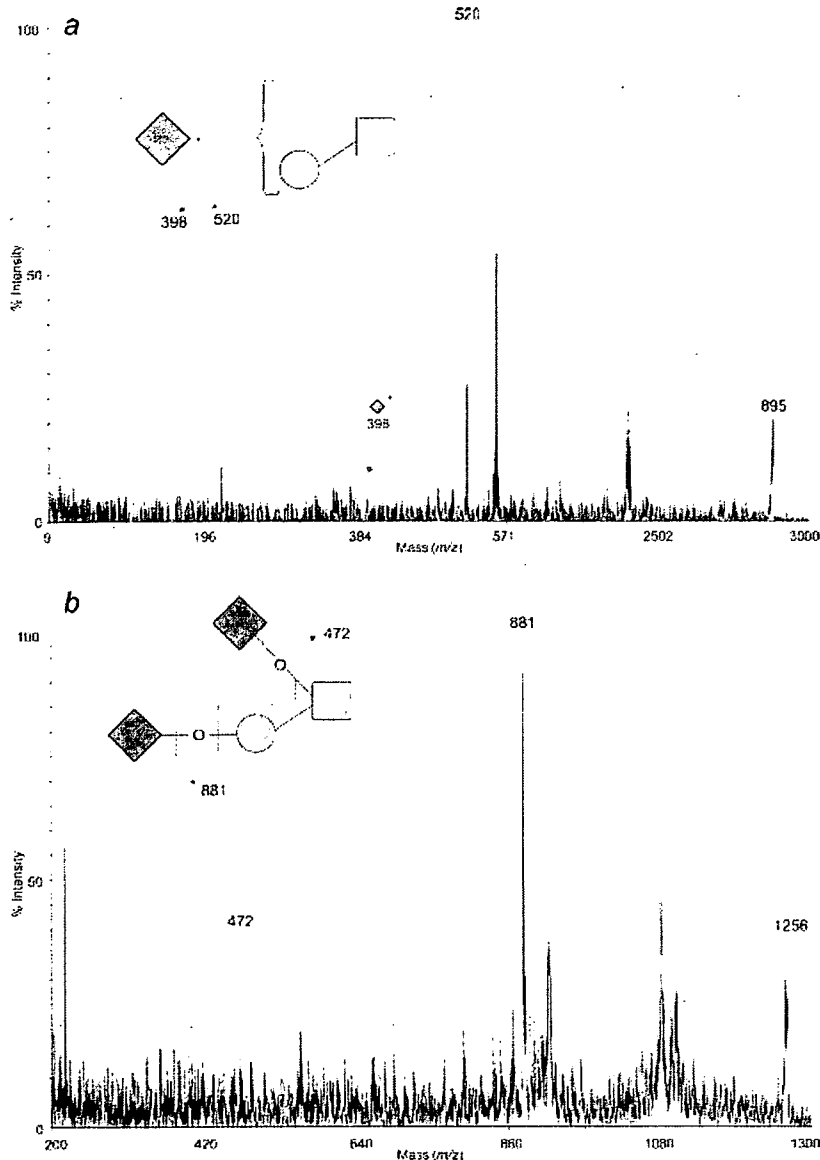


FIGURE 7 – MALDI-TOF/TOF MS/MS spectra of the signals at m/z 895 (a) and m/z 1,256 (b) in the Figure 6 spectrum. In each case a major fragment ion is observed corresponding to loss of sialic acid. For keys, see Figure 2. [Color figure can be viewed in the online issue, which is available at www.interscience.wiley.com.]

References

- Hakomori S. Aberrant glycosylation in tumors and tumor-associated carbohydrate antigens. *Adv Cancer Res* 1989;52:257–331.
- Livingston PO, Natoli EJ, Calves MJ, Stockert E, Oettgen HF, Old LJ. Vaccines containing purified GM2 ganglioside elicit GM2 antibodies in melanoma patients. *Proc Natl Acad Sci USA* 1987;84:2911–15.
- Helling F, Shang A, Calves MJ, Zhang S, Ren S, Yu RK, Oettgen HF, Livingston PO. GD₃ vaccines for melanoma: superior immunogenicity of keyhole limpet hemocyanin conjugate vaccines. *Cancer Res* 1994;54:197–203.
- Slovin SF, Ragupathi G, Adluri S, Ungers G, Terry K, Kim S, Spassova M, Bommann WG, Fazzari M, Dantis L, Olkiewicz K, Lloyd KO, et al. Carbohydrate vaccines in cancer: immunogenicity of a fully synthetic globo H hexasaccharide conjugate in man. *Proc Natl Acad Sci USA* 1999;96:5710–15.
- Hakomori S. Tumor-associated carbohydrate antigens defining tumor malignancy: basis for development of anti-cancer vaccines. *Adv Exp Med Biol* 2001;491:369–402.
- Haglund C, Kuusela P, Jalanko H, Roberts PJ. Serum CA 50 as a tumor marker in pancreatic cancer: a comparison with CA 19-9. *Int J Cancer* 1987;39:477–81.
- Hanisch FG, Uhlenbruck G, Peter-Katalinic J, Egge H. Structural studies on oncofetal carbohydrate antigens (Ca 19-9, Ca 50, and Ca 125) carried by O-linked sialyloligosaccharides on human amniotic mucins. *Carbohydr Res* 1988;178:29–47.
- Magnani JL, Nilsson B, Brockhaus M, Zopf D, Steplewski Z, Koprowski H, Ginsburg V. A monoclonal antibody-defined antigen associated with gastrointestinal cancer is a ganglioside containing sialylated lacto-N-fucopentaose II. *J Biol Chem* 1982;257:14365–9.
- Fukushi Y, Nudelman ED, Levery SB, Higuchi T, Hakomori S. A novel disialoganglioside (IV³NeuAcIII⁶NeuAcLc₆) of human adenocarcinoma and the monoclonal antibody (FH9) defining this disialosyl structure. *Biochemistry* 1986;25:2859–66.
- Stroud MR, Levery SB, Nudelman ED, Salyan MEK, Towell JA, Roberts CE, Watanabe M, Hakomori S. Extended type 1 chain glycosphingolipids: Dimeric Le^a (III⁴V³Fuc₂Lc₆) as human tumor-associated antigen. *J Biol Chem* 1991;266:8439–46.
- Watanabe M, Ohishi T, Kuzuoka M, Nudelman ED, Stroud MR, Kubota T, Kodaira S, Abe O, Hirohashi S, Shimamoto Y, Hakomori S.

- In vitro* and *in vivo* antitumor effects of murine monoclonal antibody NCC-ST-421 reacting with dimeric Lea (Lea/Lea) epitope. *Cancer Res* 1991;51:2199-204.
12. Springer GF. T and Tn, general carcinoma autoantigens. *Science* 1984;224:1198-206.
 13. Hirohashi S, Clausen H, Yamada T, Shimosato Y, Hakomori S. Blood group A cross-reacting epitope defined by monoclonal antibodies NCC-LU-35 and -81 expressed in cancer of blood group O or B individuals: its identification as Tn antigen. *Proc Natl Acad Sci USA* 1988;85:2214-20.
 14. Kjeldsen TB, Clausen H, Hirohashi S, Ogawa T, Iijima H, Hakomori S. Preparation and characterization of monoclonal antibodies directed to the tumor-associated O-linked associated O-linked sialosyl-2-6 alpha-N-acetylgalactosaminyl (sialosyl-Tn) epitope. *Cancer Res* 1988;48:2214-20.
 15. Kurosaka A, Kitagawa H, Fukui S, Numata Y, Nakada H, Funakoshi I, Kawasaki T, Ogawa T, Iijima H, Yamashina I. A monoclonal antibody that recognizes a cluster of a disaccharide, NeuAca2-6GalNAc, in mucin-type glycoproteins. *J Biol Chem* 1988;263:8724-6.
 16. Ito A, Levery SB, Saito S, Satoh M, Hakomori S. A novel ganglioside isolated from renal cell carcinoma. *J Biol Chem* 2001;276:16695-703.
 17. Saito S, Egawa S, Endoh M, Ueno S, Ito A, Numahata K, Satoh M, Kuwano S, Baba S, Hakomori S, Arai Y. RM2 antigen (beta1,4-GalNAc-disialyl-Lc4) as a new marker for prostate cancer. *Int J Cancer* 2005;115:105-13.
 18. Langlois MR, Delanghe JR. Biological and clinical significance of haptoglobin polymorphism in humans. *Clin Chem* 1996;42:1589-600.
 19. Turner GA. Haptoglobin. A potential reporter molecule for glycosylation changes in disease. *Adv Exp Med Biol* 1995;376:231-8.
 20. Mineki R, Taka H, Fujimura T, Kikkawa M, Shindo N, Murayama K. *In situ* alkylation with acrylamide for identification of cysteinyl residues in proteins during one- and two-dimensional sodium dodecyl sulphate-polyacrylamide gel electrophoresis. *Proteomics* 2002;2:1672-81.
 21. Liao CY, Chang TM, Pan JP, Chen WL, Mao SJ. Purification of human plasma haptoglobin by hemoglobin-affinity column chromatography. *J Chromatogr B Analyt Technol Biomed Life Sci* 2003;790:209-16.
 22. Brune DC. Alkylation of cysteine with acrylamide for protein sequence analysis. *Anal Biochem* 1992;207:285-90.
 23. Nishimura S, Niikura K, Kuroguchi M, Matsushita T, Fumoto M, Hinou H, Kamitani R, Nakagawa H, Deguchi K, Miura N, Monde K, Kondo H. High-throughput protein glycomics: combined use of chemoselective glycoblotting and MALDI-TOF/TOF mass spectrometry. *Angew Chem Int Ed Engl* 2004;44:91-6.
 24. Shimaoka H, Kuramoto H, Furukawa J, Miura Y, Kuroguchi M, Kita Y, Hinou H, Shinohara Y, Nishimura S. One-pot solid-phase glycoblotting and probing by transoximization for high-throughput glycomics and glycoproteomics. *Chemistry* 2007;13:1664-73.
 25. Furukawa J, Miura Y, Kuramoto H, Shimaoka H, Kuroguchi M, Nakano M, Shinohara Y, Nishimura S. Combined use of hydrazide functionalized polymer and sequential tag exchange: a general protocol with glycoblotting for functional glycomics (part 2) [Abstract no.1185]. *Glycobiology* 2006;16:1139.
 26. Miura Y, Shinohara Y, Furukawa J, Nagahori N, Nishimura S. Rapid and simple solid-phase esterification of sialic acid residues for quantitative glycomics by mass spectrometry. *Chemistry* 2007;13:4797-4804.
 27. Uematsu R, Furukawa J, Nakagawa H, Shinohara Y, Deguchi K, Monde K, Nishimura S. High throughput quantitative glycomics and glycoform-focused proteomics of murine dermis and epidermis. *Mol Cell Proteomics* 2005;4:1977-89.
 28. Wada Y, Tajiri M, Yoshida S. Hydrophilic affinity isolation and MALDI multiple-stage tandem mass spectrometry of glycopeptides for glycoproteomics. *Anal Chem* 2004;76:6560-5.
 29. Sutton-Smith M, Dell A. *Cell biology: a laboratory handbook*. San Diego, CA: Academic Press, 2005.
 30. Thompson S, Turner GA. Elevated levels of abnormally-fucosylated haptoglobins in cancer sera. *Br J Cancer* 1987;56:605-10.
 31. Thompson S, Dargan E, Griffiths ID, Kelly CA, Turner GA. The glycosylation of haptoglobin in rheumatoid arthritis. *Clin Chim Acta* 1993;220:107-14.
 32. Hay ED. The mesenchymal cell, its role in the embryo, and the remarkable signaling mechanisms that create it. *Dev Dyn* 2005;233:706-20.
 33. Lee JM, Dedhar S, Kalluri R, Thompson EW. The epithelial-mesenchymal transition: new insights in signaling, development; and disease. *J Cell Biol* 2006;172:973-81.
 34. Blanchard D, Cartron JP, Fournet B, Montreuil J, van Halbeek H, Vliegthart JF. Primary structure of the oligosaccharide determinant of blood group Cad specificity. *J Biol Chem* 1983;258:7691-5.
 35. Boffey J, Nicholl D, Wagner ER, Townson K, Goodyear C, Furukawa K, Conner J, Willison HJ. Innate murine B cells produce anti-disialosyl antibodies reactive with *Campylobacter jejuni* LPS and gangliosides that are polyreactive and encoded by a restricted set of unmutated V genes. *J Neuroimmunol* 2004;152:98-111.
 36. Kossowska B, Ferens-Sieczkowska M, Gancarz R, Passowicz-Muszynska E, Jankowska R. Fucosylation of serum glycoproteins in lung cancer patients. *Clin Chem Lab Med* 2005;43:361-9.
 37. Ang IL, Poon TC, Lai PB, Chan AT, Ngai SM, Hui AY, Johnson PJ, Sung JJ. Study of serum haptoglobin and its glycoforms in the diagnosis of hepatocellular carcinoma: a glycoproteomic approach. *J Proteome Res* 2006;5:2691-700.
 38. Ahmed N, Barker G, Oliva KT, Hoffmann P, Riley C, Reeve S, Smith AI, Kemp BE, Quinn MA, Rice GE. Proteomic-based identification of haptoglobin-1 precursor as a novel circulating biomarker of ovarian cancer. *Br J Cancer* 2004;91:129-40.
 39. Bharti A, Ma PC, Maulik G, Singh R, Khan E, Skarin AT, Salgia R. Haptoglobin alpha-subunit and hepatocyte growth factor can potentially serve as serum tumor biomarkers in small cell lung cancer. *Anticancer Res* 2004;24:1031-8.
 40. Okuyama N, Ide Y, Nakano M, Nakagawa T, Yamanaka K, Moriwaki K, Murata K, Ohigashi H, Yokoyama S, Eguchi H, Ishikawa O, Ito T, et al. Fucosylated haptoglobin is a novel marker for pancreatic cancer: a detailed analysis of the oligosaccharide structure and a possible mechanism for fucosylation. *Int J Cancer* 2006;118:2803-8.
 41. Easton RL, Patankar MS, Clark GF, Morris HR, Dell A. Pregnancy-associated changes in the glycosylation of tamm-horsfall glycoprotein. Expression of sialyl Lewis (x) sequences on core 2 type O-glycans derived from uromodulin. *J Biol Chem* 2000;275:21928-38.
 42. Buck CA, Glick MC, Warren L. Effect of growth on the glycoproteins from the surface of control and Rous sarcoma virus transformed hamster cells. *Biochemistry* 1971;10:2176-80.
 43. Ogata S, Muramatsu T, Kobata A. New structural characteristic of the large glycopeptides from transformed cells. *Nature* 1976;259:580-2.
 44. Yamashita K, Ohkura T, Tachibana Y, Takasaki S, Kobata A. Comparative study of the oligosaccharides released from baby hamster kidney cells and their polyoma transformant by hydrazinolysis. *J Biol Chem* 1984;259:10834-40.
 45. Seelentag WKF, Li W-P, Schmitz S-FH, Metzger U, Aeberhard P, Heitz PU, Roth J. Prognostic value of b1,6-branched oligosaccharides in human colorectal carcinoma. *Cancer Res* 1998;58:5559-64.
 46. Cummings RD, Kornfeld S. Characterization of structural determinants required for the high-affinity interaction of asparagine-linked oligosaccharides with immobilized *Phaseolus vulgaris* leucoagglutinating and erythroagglutinating lectins. *J Biol Chem* 1982;257:11230-4.
 47. Bierhuizen MF, Tedzes H, Schiphorst WE, van den Eijnden DH, van Dijk W. Effect of alpha2-6-linked sialic acid and alpha1-3-linked fucose on the interaction of N-linked glycopeptides and related oligosaccharides with immobilized *Phaseolus vulgaris* leucoagglutinating lectin (L-PHA). *Glycoconj J* 1988;5:85-97.
 48. Schachter H. Biosynthetic controls that determine the branching and microheterogeneity of protein-bound oligosaccharides. *Biochem Cell Biol* 1986;64:163-81.
 49. Kang R, Saito H, Ihara Y, Miyoshi E, Koyama N, Sheng Y, Taniguchi N. Transcriptional regulation of the *N*-acetylglucosaminyltransferase V gene in human bile duct carcinoma cells (HuCC-T1) is mediated by Ets-1. *J Biol Chem* 1996;271:26706-12.
 50. Pierce M, Buckhaults P, Chen L, Fregien N. Regulation of *N*-acetylglucosaminyltransferase V and Asn-linked oligosaccharide beta(1,6) branching by a growth factor signaling pathway and effects on cell adhesion and metastatic potential. *Glycoconj J* 1997;14: 623-30.

Epigenetic Modifications of *RASSF1A* Gene through Chromatin Remodeling in Prostate Cancer

Ken Kawamoto,¹ Steven T. Okino,¹ Robert F. Place,¹ Shinji Urakami,¹ Hiroshi Hirata,¹ Nobuyuki Kikuno,^{1,2} Toshifumi Kawakami,¹ Yuichiro Tanaka,¹ Deepa Pookot,¹ Zhong Chen,¹ Shahana Majid,¹ Hideki Enokida,³ Masayuki Nakagawa,³ and Rajvir Dahiya¹

Abstract Purpose: The RAS-association domain family 1, isoform A (*RASSF1A*) gene is shown to be inactivated in prostate cancers. However, the molecular mechanism of silencing of the *RASSF1A* gene is not fully understood. The present study was designed to investigate the mechanisms of inactivation of the *RASSF1A* gene through the analysis of CpG methylation and histone acetylation and H3 methylation associated with the *RASSF1A* promoter region.

Experimental Design: Methylation status of the *RASSF1A* gene was analyzed in 131 samples of prostate cancer, 65 samples of benign prostate hypertrophy (BPH), and human prostate cell lines using methylation-specific PCR. Histone acetylation (acetyl-H3, acetyl-H4) and H3 methylation (dimethyl-H3-K4, dimethyl-H3-K9) status associated with the promoter region in prostate cells were analyzed by chromatin immunoprecipitation (ChIP) assay.

Results: Aberrant methylation was detected in 97 (74.0%) prostate cancer samples and 12 (18.5%) BPH samples. The methylation frequency of *RASSF1A* showed a significant increase with high Gleason sum and high stage. The ChIP assays showed enhancement of histone acetylation and dimethyl-H3-K4 methylation on the unmethylated *RASSF1A* promoter. TSA alone was unable to alter key components of the histone code. However, after 5-aza-2'-deoxy-cytidine treatment, there was a complete reversal of the histone components in the hypermethylated promoter. Levels of acetyl-H3, acetyl-H4, and dimethyl-H3-K4 became more enriched, whereas H3K9me2 levels were severely depleted.

Conclusions: This is the first report suggesting that reduced histone acetylation or H3K4me2 methylation and increased dimethyl-H3-K9 methylation play a critical role in the maintenance of promoter DNA methylation-associated *RASSF1A* gene silencing in prostate cancer.

Prostate cancer is the most commonly diagnosed malignancy and the second leading cause of cancer-related deaths among men in the United States and Europe (1). The incidence of prostate cancer increases with aging (2). Once a tumor has metastasized, the long-term prognosis is poor because no curative therapy is available. Cancer development and metastasis are multistep processes that, among others,

involve the inactivation of tumor suppressor genes. When normal expression levels of these growth-inhibitory proteins are suppressed, uncontrolled cell cycling and growth can result. Identifying such specific molecular changes may contribute to improved diagnosis, clinical management, and outcome prediction of newly diagnosed prostate cancers (3).

Silencing of cancer-associated genes by hypermethylation of CpG islands within the promoter and/or 5' regions is a common feature of human cancer and is often associated with partial or complete transcriptional block (4). This epigenetic alteration provides an alternative pathway to gene silencing in addition to gene mutation or deletion. Moreover, the finding of promoter methylation of several genes in small biopsies and bodily fluids of cancer patients has proven to be useful as a molecular tool for cancer detection (5, 6).

The RAS-association domain family 1 has seven different isoforms that are produced by alternative splicing and transcription from two different promoters with CpG islands (7, 8). The RAS-association domain family 1, isoform A (*RASSF1A*) gene is a tumor suppressor gene in the RAS pathway that can regulate proliferation, induce apoptosis, and bind to and stabilize microtubules (9). Inactivation of *RASSF1A* is frequently observed in a number of solid tumors and epithelial cancers, including prostate cancer (3, 10–17).

Authors' Affiliations: ¹Department of Urology, Veterans Affairs Medical Center and University of California School of Medicine, San Francisco, California; ²Department of Urology, Shimane University, Faculty of Medicine, Izumo 693-8501, Japan; and ³Department of Urology, Graduate School of Medical and Dental Sciences, Kagoshima University, Kagoshima 890-8520, Japan
Received 9/6/06; revised 2/2/07; accepted 2/16/07.

Grant support: NIH grants R01CA101844, R01CA111470, R01CA108612, R01AG21418, and T32DK07790, VA Merit Review and Research and Engineering Apprenticeship Program grants.

The costs of publication of this article were defrayed in part by the payment of page charges. This article must therefore be hereby marked *advertisement* in accordance with 18 U.S.C. Section 1734 solely to indicate this fact.

Requests for reprints: Rajvir Dahiya, Urology Research Center (112F), Veterans Affairs Medical Center and University of California School of Medicine, San Francisco, 4150 Clement Street, San Francisco, CA 94121. Phone: 415-750-6964; E-mail: rdahiya@urology.ucsf.edu.

© 2007 American Association for Cancer Research.
doi:10.1158/1078-0432.CCR-06-2225

In the present study, we investigated the chromatin changes involved in the inactivation of the *RASSF1A* gene in prostate cancer samples through the analysis of CpG methylation in the promoter regions, histone acetylation (acetyl-H3, acetyl-H4), dimethyl-H3-K4 (H3K4me2), and dimethyl-H3-K9 (H3K9me2) methylation associated with the *RASSF1A* promoter region.

Materials and Methods

Clinical samples. A total of 131 newly diagnosed prostate cancer tissues from radical prostatectomy and 65 pathologically proven benign prostate hypertrophy (BPH) samples from transurethral resection (TUR-P). The pathologic background of the prostate cancer patients included Gleason sum (GS) <7 (75 cases) and GS \geq 7 (56 cases); pT2 (85 cases), pT3 (44 cases), and pT4 (2 cases); and preoperative serum PSA <4.0 (18 cases), PSA 4.0-10.0 (63 cases), and PSA >10.0 (50 cases). The median follow-up time was 35.5 months, with a range from 0.7 to 91.4 months. Serum PSA levels after radical prostatectomy was used as a surrogate end point, with a level \geq 0.2 ng/mL designated as PSA failure. The median age of prostate cancer and BPH patients was 70 years (49-80 years) and 75 years (54-87 years), respectively. The pathologic findings of prostate cancer samples were decided by the general rule for Clinical and Pathological Studies on Prostate Cancer by the Japanese Urological Association and the Japanese Society of Pathology (18). The routine strategy to diagnose prostate cancer included serum PSA level, transrectal ultrasonography, color Doppler ultrasonography, and MRI, which allowed accurate localization of prostate cancer before radical prostatectomy (19). Each tissue sample was fixed in 10% buffered formalin (pH 7.0) and embedded in paraffin wax. For histologic evaluation, 5- μ m-thick sections were used for H&E staining. All of the samples were microscopically dissected and analyzed for methylation (20). In BPH samples, high-grade prostate intraepithelial neoplasia and cancer were ruled out by microscopic analysis.

Cell lines. RWPE-1 and PWR-1E, a nontumorigenic human prostatic epithelial cell line, and the human prostate cancer cell lines LNCaP and PC3 were obtained from the American Type Culture Collection. RWPE-1 and PWR-1E cells were maintained in keratinocyte serum-free medium (Life Technologies) supplemented with 50 μ g/mL bovine pituitary extract, 5% L-glutamine, and 5 ng/mL epidermal growth factor. Both prostate cancer cell lines were maintained in RPMI 1640 with L-glutamine and sodium pyruvate. The cells were maintained in a humidified incubator (5% CO₂) at 37°C.

Nucleic acid extraction. Genomic DNA was extracted from cell lines, prostate cancer, and control prostate samples using a QIAamp DNA Mini Kit (Qiagen) after microdissection (20). The concentrations of DNA and RNA were determined spectrophotometrically, and their integrity was assessed by gel electrophoresis.

Methylation analysis. Genomic DNA from all prostate samples (100 ng) was subjected to sodium bisulfite modification using a CpGenome DNA Modification Kit (Intergen Co.). The methylation status of the promoter region of *RASSF1A* was analyzed by methylation-specific PCR (MSP) as described previously (21). The first universal primer set (PAN) covers no CpG sites in either the forward or reverse primer and amplifies a DNA fragment of the promoter region containing a number of CpG sites. Then, a second round of nested MSP or unmethylation-specific PCR (USP) was done using the universal PCR products as templates. Referring to a previous report (22), primer sequences were designed for MSP and USP. The primer sequences and PCR conditions are shown in Table 1. For semiquantitative analysis, a preliminary suitable number of PCR cycles for each MSP and USP were carried out to determine the linear range of the reaction. In each assay, the absence of DNA template served as negative control. CpGenome Universal Methylated DNA (Intergen) was used as a positive control for methylated alleles. The obtained MSP and USP products were analyzed by electrophoresis in 3% agarose gels and stained with ethidium bromide.

Bisulfite DNA sequencing. Bisulfite-modified DNA was amplified using a pair of universal primers. Direct bisulfite DNA sequencing of the PCR products using either forward universal primer or reverse primer was done according to the manufacturer's instructions (Applied Biosystems).

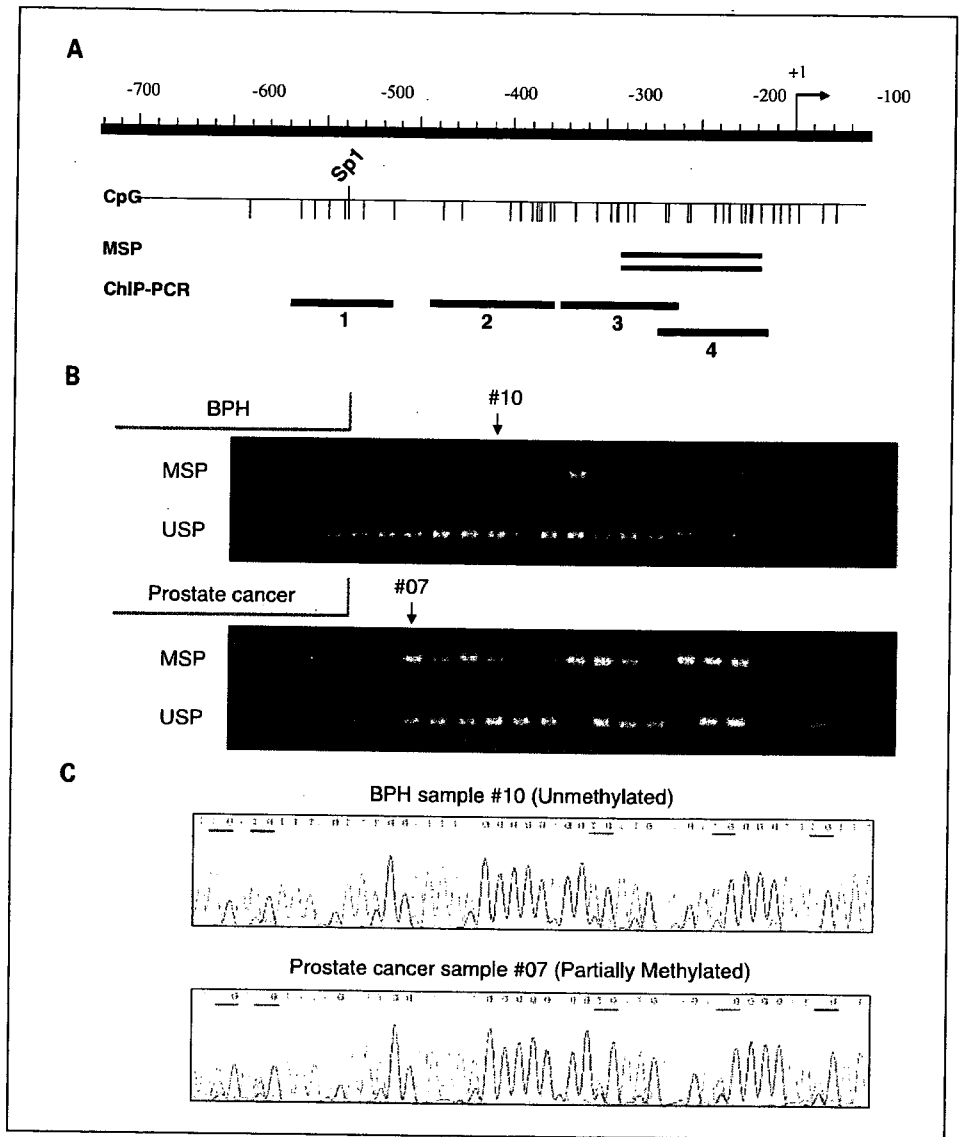
5'-aza-2'-deoxycytidine and TSA treatment. Cells were treated with the DNA methyltransferase inhibitor 5-aza-2'-deoxy-cytidine (5-aza-dC; Sigma-Aldrich) at 5 μ mol/L for 48 h and/or the histone deacetylase (HDAC) inhibitor trichostatin A (TSA, Upstate Biotechnology) at 300 nmol/L for 24 h. The genomic DNA and total RNA were extracted from the cell lines before and after drug treatment and were used for MSP and reverse transcription-PCR (RT-PCR; TITANIUM One-Step RT-PCR kit, BD Biosciences). The primer sequences (22) and PCR conditions are shown in Table 1.

Chromatin immunoprecipitation assay. Chromatin immunoprecipitation (ChIP) assays were done on cell line DNA using a EZ ChIP (Upstate Biotechnology) and followed the manufacturer's protocols with some modifications. Formaldehyde was added to the cells in a culture dish to a final concentration of 1% and incubated at 37°C for 10 min. The cells were washed in 1 mL of ice-cold PBS with proteinase inhibitors, scraped, and resuspended in 400 μ L of SDS lysis buffer. Lysates were sonicated for 10 s nine times on ice and centrifuged at 15,000 rpm for 10 min at 4°C. Supernatants were

Table 1. Primer sequences and PCR conditions

	Sense primer (5' → 3')	Antisense primer (5' → 3')	Annealing temperature (°C), PCR cycles	Product size (bp)
MSP primers				
PAN	GGAGGGAAGGAAGGGTAAG	CAACTCAATAAACTCAAACCTCCC	54, 40	260
MSP	GGGTTTTGCGAGAGCGCG	GCTAACAAACGCGAACCG	64, 35	169
USP	GGTTTTGTGAGAGTGTGTTTAG	CACTAACAAACACAAACCAAC	60, 35	169
RT-PCR primers				
<i>RASSF1A</i>	CAGATTGCAAGTTCACCTGCCACTA	GATGAAGCCTGTGTAAGAACCGTCCT	60, 33	242
<i>GAPDH</i>	GAGTCAACGGATTGGTCTGT	TGGAATCATATTGGAACATGTAAA	60, 32	135
ChIP primers				
1	GATCACGGTCCAGCCTCTGC	CTCGAGCCTTCACTTGGGGT	60, 32	109
2	GCTTCAGCAAACCGGACCGAGG	CCGGACGGCCACAACGA	60, 32	134
3	TGGGGTGTGAGGAGGGGACGA	AGAGCCGCGCAATGGA	60, 32	124
4	GTTCCATTGCGCGGCTCT	CTGGCTTGGGCGCTAGCAAG	60, 32	124
<i>GAPDH</i>	TACTAGCGGTTTTACGGGCG	TGAAACAGGAGGAGCAGAGAGCGGA	60, 32	166

Fig. 1. *A*, schematic representation of the promoter region of the human *RASSF1A* gene. Vertical lines, location of CpG dinucleotides; arrow, approximate position of the transcription start site. Doubled horizontal line, region examined by MSP. Four horizontal bars, location of the DNA fragments amplified by PCR done on the DNA recovered from ChIP assay. *B*, typical MSP results in BPH and prostate cancer samples are shown. Methylated bands were detected in 97 (74.0%) of the prostate cancer samples and in only 12 (18.5%) of the BPH samples. *C*, bisulfite DNA sequencing of unmethylated (*top*) and partially methylated (*bottom*) samples. In unmethylated samples, every CpG site was unmethylated. In partially methylated samples, there was a "T" peak along with a "C" peak at the CpG sites. Bars under the sequence, CpG sites. The results of the bisulfite DNA sequencing were consistent with those obtained by MSP.



loaded on 1% agarose gels and determined to have reduced DNA lengths between 200 and 1,000 bp. The sonicated samples were precleared with salmon sperm DNA/protein A agarose beads (Upstate Biotechnology). The soluble chromatin fraction was collected, and 8 μ L of antibody for acetyl-H3, acetyl-H4, dimethyl-H3-K4 (H3K4me2), or 12 μ L of antibody for dimethyl-H3-K9 (H3K9me2), or no antibody, was added and incubated overnight with rotation (23). All antibodies were purchased from Upstate Biotechnology. After rotation, chromatin-antibody complexes were collected using salmon sperm DNA/protein A agarose beads and washed according to the manufacturer's protocol. Immunoprecipitated DNA was recovered using a QIAquick PCR Purification Kit (Qiagen) and analyzed by PCR. We used previously reported (23, 24) primers designed to separately amplify four regions in the *RASSF1A* promoter area (Fig. 1A). The primer pairs used for ChIP assays are shown in Table 1. One additional primer set was used to amplify a 166-bp fragment of the glyceraldehyde-3-phosphate dehydrogenase (*GAPDH*) gene as an internal control. Each PCR reaction was initially set up using different amounts of ChIP sample with varying PCR cycle numbers, and we selected the final PCR conditions accordingly. PCR products were analyzed on 3.0% agarose gels and visualized by UV illumination. Densitometric analysis

of the observed bands was done using ImageJ software.⁴ Relative enrichment was calculated by taking the ratio between the net intensity of the *RASSF1A* PCR product from each primer set and the net intensity of the *GAPDH* PCR product for the bound sample and dividing this by the same ratio calculated for the input sample (25). The value of each point was calculated as the average from two independent ChIP experiments and a total of four independent PCR analyses.

Statistical analysis. The relationship between clinicopathologic findings and methylation status of the *RASSF1A* gene was done using the χ^2 test and Fisher's exact test. For each clinicopathologic finding, the association with PSA failure-free probability was determined using Kaplan-Meier curves, and a log-rank test was used to determine significance. *P* values of <0.05 were regarded as statistically significant. All statistical analyses were done using StatView version 5.0 for Windows.

⁴ <http://rsb.info.nih.gov/ij>

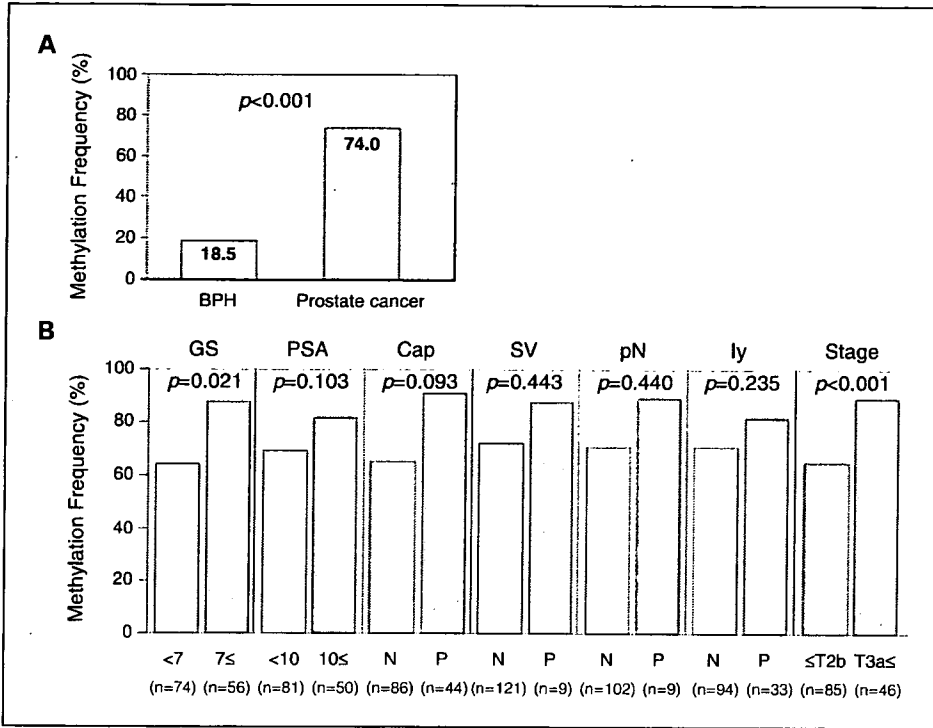


Fig. 2. Correlation of clinicopathologic features with methylation frequency of the *RASSF1A* promoter. **A**, the difference in the frequency of *RASSF1A* promoter methylation was significant between prostate cancer and BPH samples. **B**, there was significant correlation between methylation frequency of *RASSF1A* and high GS or clinical stage. Methylation frequency of *RASSF1A* increased with higher GS and high stage. The total number of patients was 131, but some patients were lacking clinicopathologic findings, and then data were not included. Cap, capsular invasion; SV, seminal vesicle involvement; pN, lymph node invasion; ly, lymphatic vessel invasion. N and P, negative and positive, respectively.

Results

Methylation status of *RASSF1A* gene. Typical examples of MSP and USP bands obtained during methylation analysis of the *RASSF1A* promoter are shown in Fig. 1B. To confirm the methylation status of the *RASSF1A* promoter, bisulfite-modified DNA was amplified and sequenced. Typical bisulfite-

modified DNA sequencing of prostate cancer and BPH samples are shown in Fig. 1C. In BPH samples, most CpG sites were not methylated, whereas in prostate cancer samples, most CpG sites were methylated in the promoter region. In the total group of prostate cancer and BPH, there was no correlation between age and methylation. In the 131 prostate cancer samples, positive *RASSF1A* methylation was detected in 97

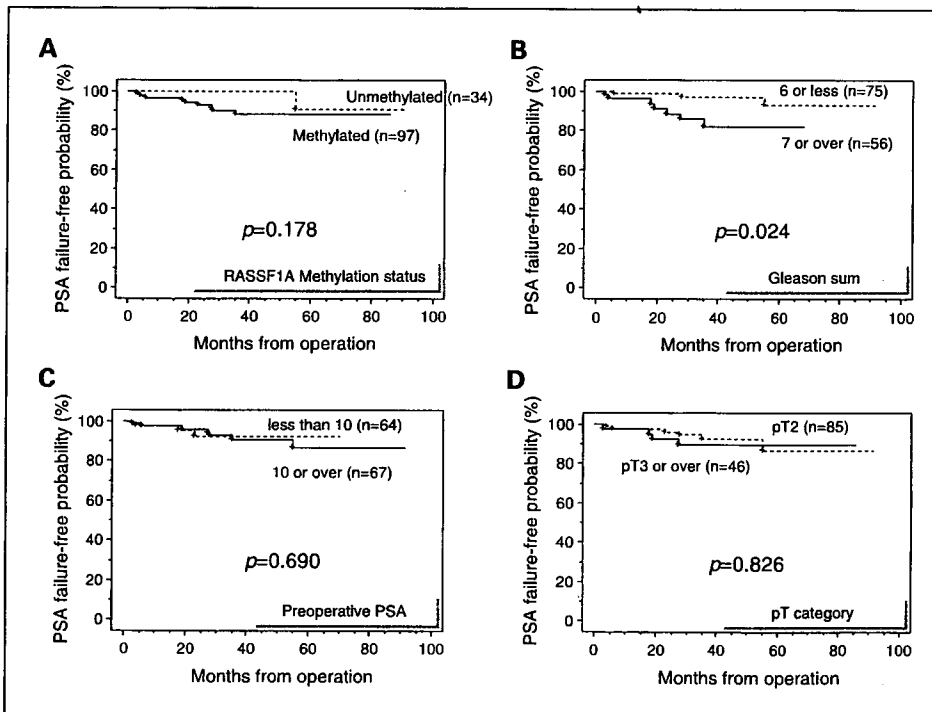
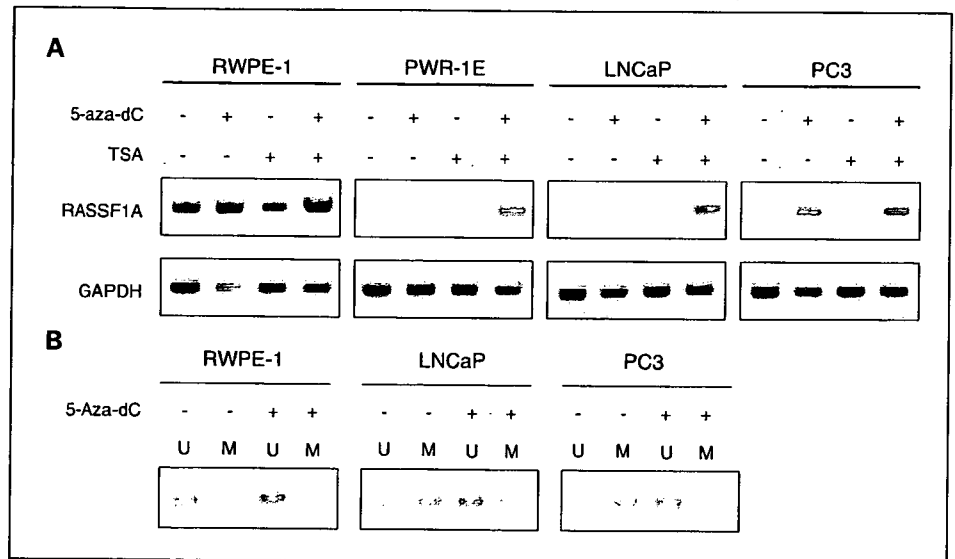


Fig. 3. Kaplan-Meier PSA failure-free survival curves of prostate cancer patients after radical prostatectomy, grouped according to the evaluated variables. **A**, methylation frequency of *RASSF1A*; **B**, GS; **C**, preoperative PSA; **D**, pT category. Follow-up ranged from 0.7 to 91.4 mo, with a median of 35.5 mo.

Fig. 4. A. RT-PCR analysis of *RASSF1A* expression in a normal prostatic epithelial cell lines and two prostate cancer cell lines. The mRNA transcript of *RASSF1A* was significantly increased after 5-aza-dC treatment alone or with a combination of 5-aza-dC and TSA in PWR-1E and the two cancer cell lines. In contrast, TSA treatment failed to re-express the *RASSF1A* gene in these cell lines. *GAPDH* expression served as a loading control. **B.** MSP analysis of *RASSF1A*. MSP analysis showed partial demethylation of the *RASSF1A* promoter region after 5-aza-dC treatment in prostate cancer cell lines. M, reactions specific for methylated DNA; U, reactions specific for unmethylated DNA.



samples (74.0%). On the other hand, in 65 BPH samples, positive *RASSF1A* methylation was detected in 12 samples (18.5%). The difference in the frequency of *RASSF1A* promoter methylation was significant between prostate cancer and BPH samples ($P < 0.001$; Fig. 2A). The methylation frequency of *RASSF1A* showed a significant increase with high GS (63% in GS < 7 , and 88% in GS ≥ 7 ; $P = 0.002$; Fig. 2B) and clinical stage (65% in stage $\leq T2b$ and 91% in stage $\geq T3a$; $P < 0.001$; Fig. 2B). Although there was a tendency toward increased *RASSF1A* promoter methylation, there was no significant association with high PSA or other pathologic categories (Fig. 2B). PSA failure-free probability was analyzed as disease-free survival, with PSA failure occurring in 10 patients (7.6%). Of the clinicopathologic features considered, only GS was significantly associated with poor outcome ($P = 0.022$; Fig. 3B).

Effects of 5-aza-dC and TSA on *RASSF1A* gene expression in prostate cancer cells. To clarify the role of epigenetic suppression of the *RASSF1A* gene, we treated prostate cancer cell lines with 5-aza-dC and TSA. At baseline, expression of the *RASSF1A* mRNA transcript was detected in the normal prostate cell line (RWPE-1), but was negative in PWR-1E and prostate cancer cell lines (LNCaP and PC3). With TSA treatment, *RASSF1A* re-expression was not detected in prostate cancer cell lines. However, the expression level was significantly increased in both prostate cancer cell lines after treatment with the demethylating agent 5-aza-dC or combined treatment with azaC and TSA (Fig. 4A). To determine the effects of the demethylating agent, we examined the methylation status in LNCaP and PC3 cells after 5-aza-dC treatment. In both cell lines, partial demethylation was detected by MSP (Fig. 4B).

ChIP assay. The association of *RASSF1A* promoter methylation and gene silencing in relation to chromatin remodeling has not been reported previously in prostate cancer. To establish this functional link, we examined local histone acetylation and H3 methylation in the chromatin associated with the *RASSF1A* promoter region using a ChIP assay. The histone-associated DNAs, immunoprecipitated with antibodies against acetyl-H3, acetyl-H4, H3K4me2, or H3K9me2, were individually amplified with four primer sets covering the

RASSF1A promoter region (Fig. 1A). The results in Fig. 5 show marked differences in the levels of histone acetylation and H3 methylation. Enhancement of histone acetylation and H3K4me2 methylation was observed in RWPE-1 cells, in which the *RASSF1A* promoter is unmethylated and transcriptionally active; however, there was no acetylation or methylation of these same sites in the hypermethylated, transcriptionally silenced promoters (PWR-1E, LNCaP, and PC3). In contrast, H3K9me2 was enriched along the entire hypermethylated and transcriptionally inactive promoters.

To investigate the effect of DNA methyltransferase inhibitor and HDAC-I in the histone modifications of *RASSF1A* promoter, we treated LNCaP cells with 5-aza-dC and/or TSA (Fig. 6A and B). The ChIP assays revealed that TSA treatment alone did not induce any alteration of histone modification. These data show that in addition to being unable to reactivate expression of a hypermethylated, silenced *RASSF1A* gene, TSA alone was unable to evoke obvious change in key parameters of the histone code in the *RASSF1A* promoter (25). In contrast, we observed a complete reversal of the histone modifications after 5-aza-dC treatment alone or the combination of 5-aza-dC and TSA. Acetyl-H3, acetyl-H4, and H3K4me2 levels were higher, whereas H3K9me2 levels were lower in the promoter region.

Discussion

Transcriptional gene silencing by hypermethylation of CpG islands in the promoter region is becoming recognized as a common mechanism for the inactivation of tumor suppressor genes in human malignancies (26–28). In recent years, the list of tumor suppressor genes that are inactivated by epigenetic events rather than classic mutation/deletion events has been growing (7). Unlike mutational inactivation, methylation is reversible, and demethylating agents and inhibitors of HDACs are being used in clinical trials (7).

DNA methylation is an important mechanism in prostate cancer and is involved in the inactivation of various essential genes such as E-cadherin (29), MDR1 (30), and glutathione S-transferase P1 (31). In this study, we found that the *RASSF1A*

gene was methylated in 74% of prostate cancer cases examined. Liu et al. (15) has also reported that *RASSF1A* methylation was frequently observed in prostate cancer (71%). *RASSF1A* functions as a tumor suppressor gene through several distinct pathways, including microtubule stability (32, 33) and cell cycle regulation (8, 16, 34). The *RASSF1A* gene has several isoforms, including *RASSF1A* and *RASSF1C* that are transcribed from two different promoters containing CpG islands (10, 11). Selective promoter methylation of the *RASSF1A* promoter, but not *RASSF1C*, is frequent in many cancers, including lung, breast, ovarian, and renal cell carcinomas (10–13). In prostate cancer, inactivation of the *RASSF1A* gene was reported to be related to carcinogenesis, and Maruyama et al. (3) described a significant correlation between methylation status, GS, PSA levels, and stage. The results of the present study also showed that *RASSF1A* promoter methylation was associated with high GS and clinical stage. Currently, Rosenbaum et al. (35) reported that the methylation status of selected genes (*GSTPI*, *APC*) in prostate cancer specimens may be predictive for time to recurrence in patients undergoing prostatectomy. We also analyzed PSA failure-free probability as disease-free survival. Of the clinicopathologic features considered, only GS was significantly associated with poor outcome.

The mechanisms of *RASSF1A* epigenetic change in relation to prostate tumorigenesis, especially chromatin structural changes during the silencing of the genes, are not known. Thus, we examined the molecular mechanisms of inactivation of the *RASSF1A* gene by analysis of chromatin remodeling such as CpG methylation in the promoter regions, histone acetylation (acetyl-H3, acetyl-H4), dimethyl-H3-K4 (H3K4me2) and dimethyl-H3-K9 (H3K9me2) methylation associated with the *RASSF1A* promoter region. Histone acetylation and H3K4me2 methylation were increased in the unmethylated RWPE-1 *RASSF1A* promoter; however, there was no acetylation or methylation of these same sites in the hypermethylated LNCaP and PC3 promoter. In contrast, H3K9me2 was enriched along the entire hypermethylated and transcriptionally inactive promoter in LNCaP and PC3 cells. Similar results has been reported in breast cancer (23, 24). These results support the idea that DNA methylation-mediated gene silencing is closely linked with repressive histone modifications at the gene promoter in cancer cells (23, 25, 36).

In this study, we also investigated the effect of a DNA methyltransferase inhibitor (5-aza-dC) and/or a HDAC-inhibitor (TSA) on chromatin remodeling. We treated LNCaP cells with TSA alone, but there was no change in histone acetylation and H3

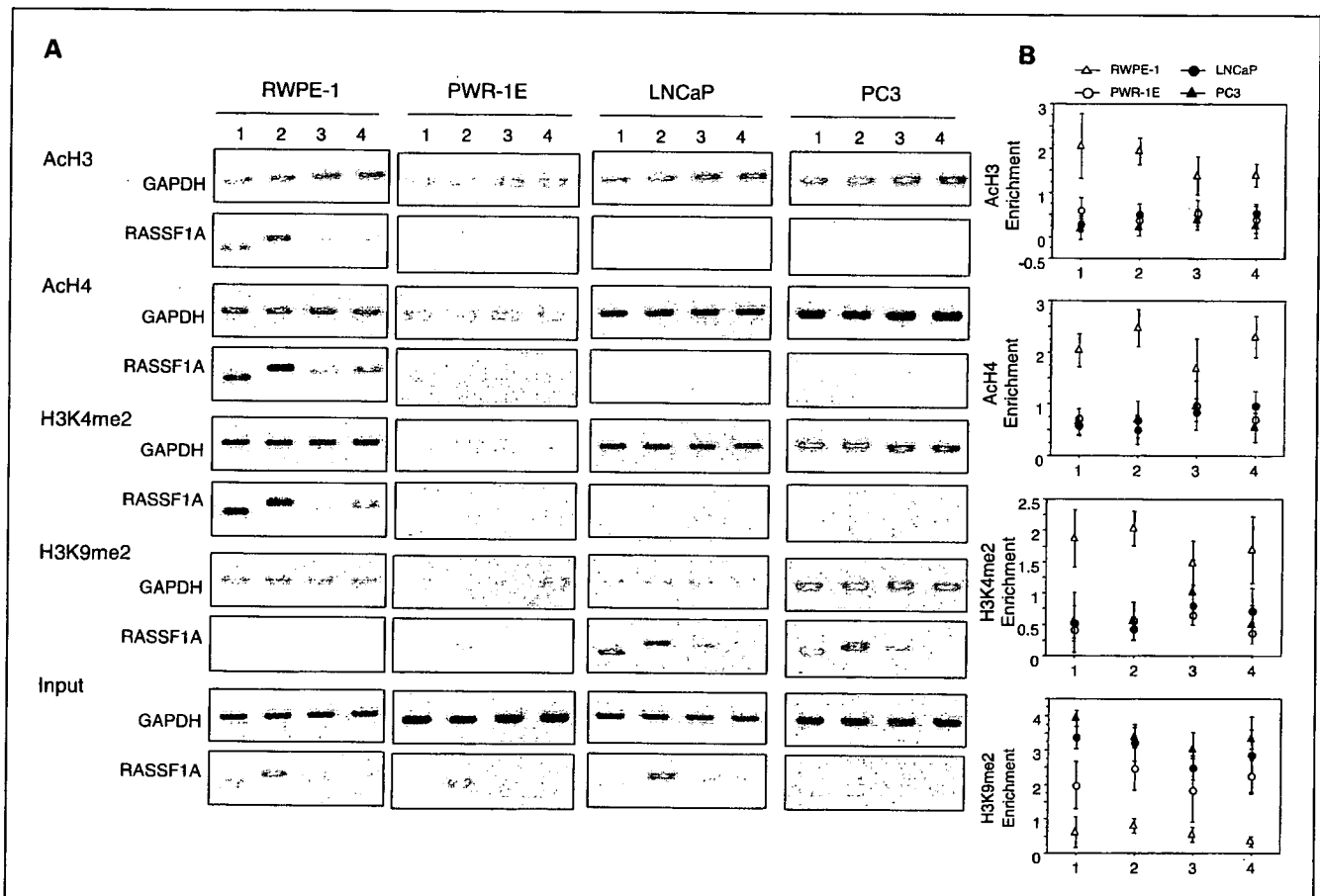


Fig. 5. ChIP assays of the *RASSF1A* CpG island. Chromatin DNA was immunoprecipitated with antibodies specific for acetyl-H3, acetyl-H4, dimethyl-H3-K4 (H3K4me2), and dimethyl-H3-K9 (H3K9me2), respectively. DNA fragments corresponding to *RASSF1A* promoter regions 1, 2, 3, and 4 (see Fig. 1A) were amplified by PCR. Enhancement of histone acetylation and H3K4me2 methylation was observed in the RWPE-1 promoter. However, there was no acetylation or methylation of these same sites in PWR-1E, LNCaP, and PC3 cells. In contrast, H3K9me2 was enriched in these cell lines. A, PCR analyses of ChIP assay on RWPE-1, PWR-1E, LNCaP, and PC3 cells in the four promoter regions. B, points, enrichment data calculated from the corresponding DNA fragments amplified by PCR; bars SD.

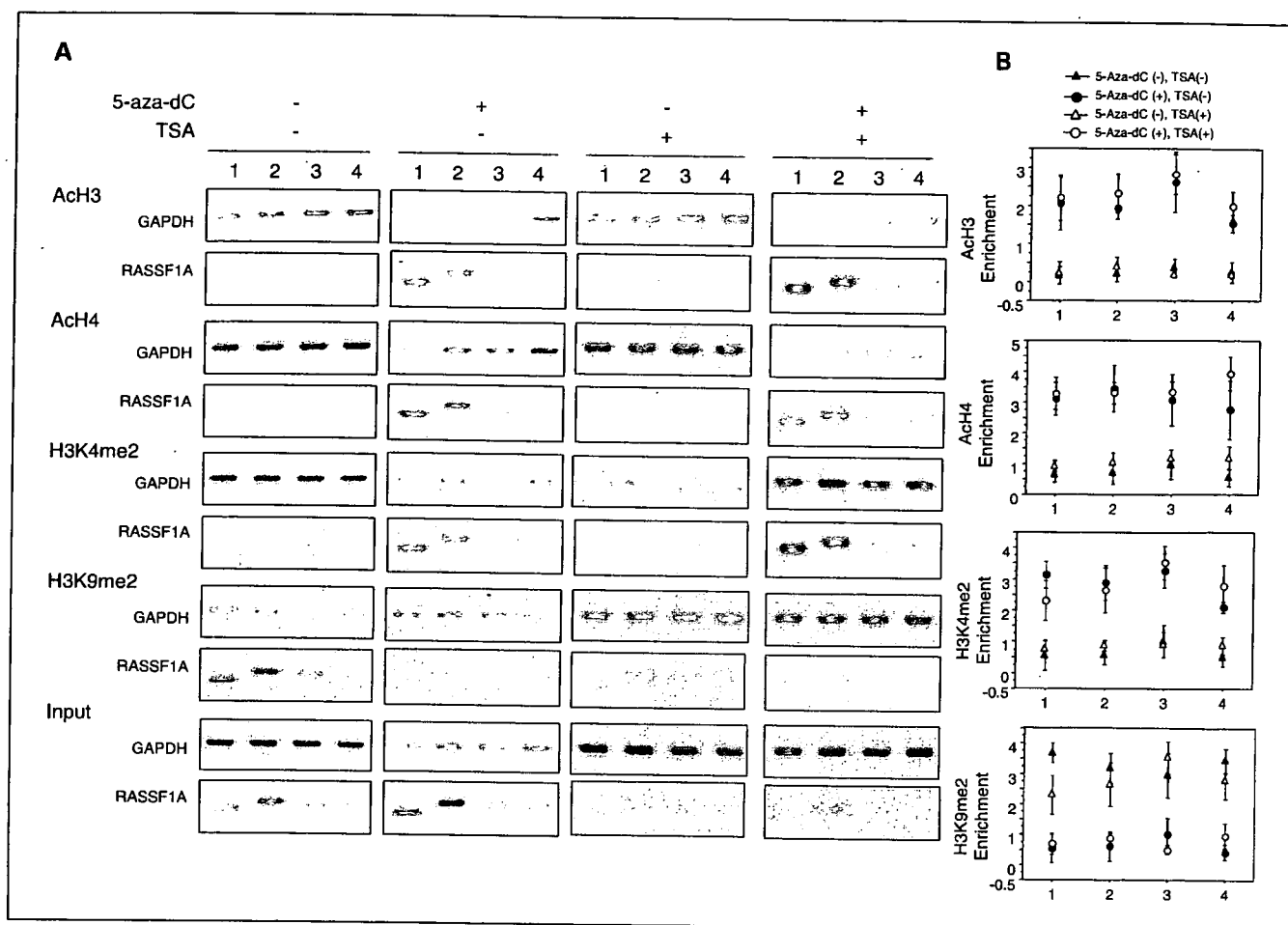


Fig. 6. Effects of 5-aza-dC and TSA on the histone modifications of the *RASSF1A* promoter. ChIP assays were done on LNCaP cells after treatment with 5 $\mu\text{mol/L}$ 5-aza-dC for 48 h and/or 300 nmol/L TSA for 24 h. TSA treatment alone did not induce any alteration of histone modification. In contrast, complete reversal of the histone modifications were observed after 5-aza-dC treatment alone or the combination of 5-aza-dC and TSA. Acetyl-H3, acetyl-H4, and H3K4me2 levels were higher, whereas H3K9me2 levels were lower in this region of the promoter. **A.** PCR analyses of ChIP assays. **B.** points, enrichment data calculated from the corresponding DNA fragments amplified by PCR; bars, SD.

methylation. In contrast, after 5-aza-dC treatment alone or a combination of 5-aza-dC and TSA, there was increased accumulation of acetylated histones and H3K4me2 methylation concomitant with reactivation of the methylated *RASSF1A* promoter. These results favor the idea that DNA methylation is more important compared with histone deacetylation in maintaining a silent state at hypermethylated promoters because 5-aza-dC can reactivate genes silenced with aberrant promoter hypermethylation, but TSA alone did not reactivate these genes (37). This change in histone modification upon inhibition of DNA methyltransferase suggests that in prostate cancer cells, DNA hypermethylation, or another activity mediated by DNA methyl-

transferase, may also be essential for maintaining repressive histone modifications at gene promoters silenced by aberrant DNA hypermethylation (25). Furthermore, the observation that 5-aza-dC can both reactivate expression of the silenced *RASSF1A* gene and completely reverse key histone modifications surrounding the gene promoter strengthens the idea that interdependence exists between these two events.

In conclusion, this is the first report suggesting that chromatin remodeling, such as reduced histone acetylation and H3K4me2 methylation, and increased H3K9me2 methylation play a critical role in the maintenance of promoter DNA methylation-associated gene silencing in prostate cancer.

References

- Jemal A, Ward E, Hao Y, Thun M. Trends in the leading causes of death in the United States, 1970–2002. *JAMA* 2005;294:1255–9.
- Perry AS, Foley R, Woodson K, Lawler M. The emerging roles of DNA methylation in the clinical management of prostate cancer. *Endocr Relat Cancer* 2006; 13:357–77.
- Maruyama R, Toyooka S, Toyooka KO, et al. Aberrant promoter methylation profile of prostate cancers and its relationship to clinicopathological features. *Clin Cancer Res* 2002;8:514–9.
- Esteller M. CpG island hypermethylation and tumor suppressor genes: a booming present, a brighter future. *Oncogene* 2002;21:5427–40.
- Jeronimo C, Henrique R, Hoque MO, et al. A quantitative promoter methylation profile of prostate cancer. *Clin Cancer Res* 2004;10:8472–8.
- Sidransky D. Emerging molecular markers of cancer. *Nat Rev Cancer* 2002;2:210–9.
- Agathangelou A, Cooper WN, Latif F. Role of the Ras-association domain family 1 tumor

- suppressor gene in human cancers. *Cancer Res* 2005; 65:3497–508.
8. Pfeifer GP, Dammann R. Methylation of the tumor suppressor gene RASSF1A in human tumors. *Biochemistry (Mosc)* 2005;70:576–83.
 9. Liu L, Broaddus RR, Yao JC, et al. Epigenetic alterations in neuroendocrine tumors: methylation of RAS-association domain family 1, isoform A and p16 genes are associated with metastasis. *Mod Pathol* 2005;18:1632–40.
 10. Burbee DG, Forgacs E, Zochbauer-Muller S, et al. Epigenetic inactivation of RASSF1A in lung and breast cancers and malignant phenotype suppression. *J Natl Cancer Inst* 2001;93:691–9.
 11. Dammann R, Li C, Yoon JH, Chin PL, Bates S, Pfeifer GP. Epigenetic inactivation of a RAS association domain family protein from the lung tumour suppressor locus 3p21.3. *Nat Genet* 2000;25:315–9.
 12. Agathangelou A, Honorio S, Macartney DP, et al. Methylation associated inactivation of RASSF1A from region 3p21.3 in lung, breast and ovarian tumours. *Oncogene* 2001;20:1509–18.
 13. Dreijerink K, Braga E, Kuzmin I, et al. The candidate tumor suppressor gene, RASSF1A, from human chromosome 3p21.3 is involved in kidney tumorigenesis. *Proc Natl Acad Sci U S A* 2001;98:7504–9.
 14. Yegnasubramanian S, Kowalski J, Gonzalgo ML, et al. Hypermethylation of CpG islands in primary and metastatic human prostate cancer. *Cancer Res* 2004; 64:1975–86.
 15. Liu L, Yoon JH, Dammann R, Pfeifer GP. Frequent hypermethylation of the RASSF1A gene in prostate cancer. *Oncogene* 2002;21:6835–40.
 16. Dammann R, Schagdarsurengin U, Seidel C, et al. The tumor suppressor RASSF1A in human carcinogenesis: an update. *Histol Histopathol* 2005;20: 645–63.
 17. Bastian PJ, Ellinger J, Wellmann A, et al. Diagnostic and prognostic information in prostate cancer with the help of a small set of hypermethylated gene loci. *Clin Cancer Res* 2005;11:4097–106.
 18. The Japanese Urological Association and Japanese Society of Pathology. General rules for clinical and pathological studies on prostate cancer. 2nd ed. Tokyo (Japan): Kanahara-shuppan Co.; 1992.
 19. Shigeno K, Igawa M, Shiina H, Kishi H, Urakami S. Transrectal colour Doppler ultrasonography for quantifying angiogenesis in prostate cancer. *BJU Int* 2003; 91:223–6.
 20. Dahiya R, Lee C, McCarville J, Hu W, Kaur G, Deng G. High frequency of genetic instability of microsatellites in human prostatic adenocarcinoma. *Int J Cancer* 1997;72:762–7.
 21. Herman JG, Graff JR, Myohanen S, Nelkin BD, Baylin SB. Methylation-specific PCR: a novel PCR assay for methylation status of CpG islands. *Proc Natl Acad Sci U S A* 1996;93:9821–6.
 22. Lo KW, Kwong J, Hui AB, et al. High frequency of promoter hypermethylation of RASSF1A in nasopharyngeal carcinoma. *Cancer Res* 2001;61:3877–81.
 23. Yan PS, Shi H, Rahmatpanah F, et al. Differential distribution of DNA methylation within the RASSF1A CpG island in breast cancer. *Cancer Res* 2003;63: 6178–86.
 24. Strunnikova M, Schagdarsurengin U, Kehlen A, Garbe JC, Stampfer MR, Dammann R. Chromatin inactivation precedes *de novo* DNA methylation during the progressive epigenetic silencing of the RASSF1A promoter. *Mol Cell Biol* 2005;25:3923–33.
 25. Fahrner JA, Eguchi S, Herman JG, Baylin SB. Dependence of histone modifications and gene expression on DNA hypermethylation in cancer. *Cancer Res* 2002;62:7213–8.
 26. Jones PA, Laird PW. Cancer epigenetics comes of age. *Nat Genet* 1999;21:163–7.
 27. Baylin SB, Herman JG. DNA hypermethylation in tumorigenesis: epigenetics joins genetics. *Trends Genet* 2000;16:168–74.
 28. Kawaguchi K, Oda Y, Saito T, et al. DNA hypermethylation status of multiple genes in soft tissue sarcomas. *Mod Pathol* 2006;19:106–14.
 29. Li LC, Zhao H, Nakajima K, et al. Methylation of the E-cadherin gene promoter correlates with progression of prostate cancer. *J Urol* 2001;166:705–9.
 30. Enokida H, Shiina H, Igawa M, et al. CpG hypermethylation of MDR1 gene contributes to the pathogenesis and progression of human prostate cancer. *Cancer Res* 2004;64:5956–62.
 31. Enokida H, Shiina H, Urakami S, et al. Ethnic group-related differences in CpG hypermethylation of the GSTP1 gene promoter among African-American, Caucasian and Asian patients with prostate cancer. *Int J Cancer* 2005;116:174–81.
 32. Mathe E. RASSF1A, the new guardian of mitosis. *Nat Genet* 2004;36:117–8.
 33. Jackson PK. Linking tumor suppression, DNA damage and the anaphase-promoting complex. *Trends Cell Biol* 2004;14:331–4.
 34. Shivakumar L, Minna J, Sakamaki T, Pestell R, White MA. The RASSF1A tumor suppressor blocks cell cycle progression and inhibits cyclin D1 accumulation. *Mol Cell Biol* 2002;22:4309–18.
 35. Rosenbaum E, Hoque MO, Cohen Y, et al. Promoter hypermethylation as an independent prognostic factor for relapse in patients with prostate cancer following radical prostatectomy. *Clin Cancer Res* 2005;11: 8321–5.
 36. Jones PA, Baylin SB. The fundamental role of epigenetic events in cancer. *Nat Rev Genet* 2002;3: 415–28.
 37. Cameron EE, Bachman KE, Myohanen S, Herman JG, Baylin SB. Synergy of demethylation and histone deacetylase inhibition in the re-expression of genes silenced in cancer. *Nat Genet* 1999;21:103–7.